INTERNATIONAL JOURNAL FOR NUMERICAL AND ANALYTICAL METHODS IN GEOMECHANICS, VOL. 21, 43–72 (1997)

CHEMO-PLASTICITY OF CLAYS SUBJECTED TO STRESS AND FLOW OF A SINGLE CONTAMINANT

T. HUECKEL

Department of Civil and Environmental Engineering, Duke University, Durham, NC 27708, U.S.A.

SUMMARY

Isothermal chemo-elasto-plasticity of clays is discussed, to describe strains induced in clay by permeation of it with a low dielectric constant organic contaminant, in the presence of stress. The strain is crucial in controlling permeability changes in chemically affected clay barriers of landfills and impoundments. The theory encompasses chemical softening or yield surface reduction, coefficient of chemical reversible expansion or contraction due to mass concentration increase, as well as chemical sensitivity of bulk plastic modulus. The experiments on chemistry and stress dependent permeability of Sarnia clay performed by Fernandez and Quigley (1985, 1991) are interpreted using this model. The numerical representations of the chemo-plastic softening function and the chemo-elastic strain function, as well as plastic bulk modulus sensitivity to concentration are evaluated for dioxane and ethanol. Specific requirements for the tests for chemo-plastic behavior of clays are discussed.

KEY WORDS: plasticity; contaminated clays; organic contaminants; chemical consolidation; chemical swelling

INTRODUCTION

It has been recognized for sometime that certain chemicals contained in hazardous waste or produced by decomposition of landfilled municipal waste may have an adverse impact on hydraulic conductivity of clay liners. Concentrated organic liquids in laboratory conditions have been reported to increase hydraulic conductivity of clay up to 10 000 times in fixed ring permeameters. If confirmed in the field scale, the problem would require serious consideration. This is true even when the water permeability of clay is initially very low and a dominant transport mechanism is molecular diffusion. In this case, when the concentration of particular organics driven by diffusion increases in the liner, so does hydraulic conductivity. As a consequence, the advective flow increases, and over time may become dominant. On the other hand, recent findings indicate also that compressive effective stress in liners, when applied during permeation may play a key role in controlling the chemically induced changes in hydraulic conductivity, as they seem to do in flexible wall permeameter tests. Mechanisms linking the two phenomena are poorly understood, while the relationship between them is far from being quantitatively established.

There are a number of mechanisms through which individual contaminants affect hydraulic conductivity, including chemical reactions such as dissolution or precipitation, and physico-chemical phenomena affecting intermolecular forces in water solutions. The focus of this paper is limited to the second category, and specifically to organic contaminants, e.g. hydro-carbons. In this case, the central physico-chemical effect causing the increase in hydraulic conductivity is believed to result in a significant reduction of the volume of adsorbed water. This occurs when

CCC 0363–9061/97/010043–30

Received 24 February 1995
Revised 9 May 1996

pore water is replaced with concentrated contaminants (mainly organic) with a low dielectric constant (< 10), and/or at elevated temperature, which dehydrate mineral surface and open new spaces for the flow of the permeant, as suggested in the past.[1–6] The dehydration seems to be combined with some tendency of the particles to reorient themselves leading to some swelling. The opening of new spaces and swelling may be inhibited by prior imposition of effective stress on soil skeleton.

This paper is focussed on volume changes in clay related to three major microstructural phenomena: desorption of adsorbed water, tendency of particles to flocculate (or reorient) and chemo-plastic strain. The first phenomenon may be viewed as a mass transfer between the solid and liquid phase. Indeed, desorption of bound water causes the collapse of clay clusters, and opening of larger pores and flow channels between them, when effective stress acting on the skeleton is not at yielding. Effective stress is a second major factor in controlling the chemically induced changes in the pore space and hydraulic conductivity through the chemo-plastic strain.[6] A mechanical loading, in-place before the inflow of some organic chemicals, may induce chemical consolidation in clay sufficient to prevent any change in its hydraulic conductivity. The amount of the compressive effective stress necessary for such healing action is clay- and permeant-specific. On the other hand, as suggested by Mitchell and Jaber[7] "it is important to note... that a decrease in effective confining stress could occur due to an increase in the level of leachate above the liner if the leachate collection system fails". In the real situations effective stress is poorly controlled, because of variability in seepage forces, in waste weight and in pore pressure arising in a landfill due to clogging of drainage system, but extreme situations can be estimated.[8]

Thus, a two way coupling between chemo-mechanical strain and hydraulic behaviour of clay is central to its performance as liner material. The role of not only mechanical but also of chemical effects in controlling hydraulic properties is of fundamental engineering importance and, as it was formulated by Fernandez and Quigley[6] "if [effective] stress is such a major ally in preventing clay barrier damage, design of liner system for containment of organic liquids should probably incorporate this concept".

In a more general framework for multi-contaminant flow through plastic porous solid, it is assumed[9] that the solid's yield surface undergoes a reduction (chemical softening) as a function of the adsorbed water shrinking idealized as inter-phase mass transfer. In this paper a simplified isothermal chemo-plasticity formulation for a single organic, water-miscible contaminant with one dominant electrochemical property, namely low dielectric constant is proposed. This allows to characterize the chemically sensitive processes ad directly related to mass concentration of the contaminant. In what follows our interest is limited to the development of the chemo-plastic model, and the mechanisms of contaminant transport will be regarded as known.

CONSTITUTIVE RELATIONSHIP FOR CHEMO-PLASTIC STRAIN DUE TO VARIABLE MASS CONCENTRATION OF A SINGLE ORGANIC CONTAMINANT

In this section we develop a model of isothermal chemo-elasto-plastic clay behaviour in the case for a single contaminant. For this formulation constitutive functions are interpreted and identified for one clay and for two water–miscible organic contaminants, following the seminal experiments by Fernandez and Quigley.[5,6] The contaminants are ethanol and dioxane, representing an intermediate and low dielectric constant liquids (respectively, 32 and 2.3). In the following section we shall interpret their results using the developed constitutive law. Finally we shall elaborate methods of characterization of material constants, and will identify the constitutive parameters.

Because of the assumption that there is only one contaminant, and at constant temperature, all the chemically induced variations in material properties will be referred to variations in the contaminant mass concentration c,

$$c = \frac{m^{\mathrm{c}}}{m^{\mathrm{f}}} \tag{1}$$

where m^{c} and m^{f} are contaminant and total fluid mass, respectively.

For dense clays, characterized by the predominance of face-to-face inter-particle contacts, the Terzaghi's effective stress principle is still valid for chemically loaded clays.[10] However, the total strain rate $\dot{\varepsilon}_{ij}$ (positive in compression) needs to include a part which is dependent on changes in the chemistry of pore liquid as discussed by Hueckel[9] and, in this case, concentration rate. Dividing the strain rate into its respective reversible and irreversible parts the total strain rate becomes

$$\dot{\varepsilon}_{ij} = C_{ijkl}(c)\,\dot{\sigma}'_{kl} - \frac{1}{3}\beta(\sigma'_{kl}, c)\,\dot{c}\,\delta_{ij} + \dot{\Lambda}(\dot{\sigma}'_{mn}, \dot{c})\,\frac{\partial f(\sigma'_{kl}, c)}{\partial \sigma'_{ij}} \tag{2}$$

where σ'_{ij} is the effective stress. The first right-hand-side term is the reversible (elastic) mechanical strain, and C_{ijkl} is the tensor of elastic compliance constants, which depends on the contaminant concentration. The second term on the right-hand side is the reversible chemical strain rate, assumed to be isotropic. Its coefficient β is a scalar function analogous to the thermal expansion coefficient. Microscopically this strain corresponds to clay volume changes being a resultant of several sometimes competing reversible structural or fabric changes induced by change in electro-chemical properties of pore liquid. These changes may be resulting from the tendency of clay particles (whole clusters or loose single platelets) to rotate to assume an edge-to-face configuration or to flocculate. Flocculation, according to Lambe,[11] and Bennett and Hulbert [12] in an unconstrained environment consists in a reorientation of particles into a random system. In a constrained environment, the final configuration may not reach an isotropic stage, but at least the rate of change of orientation is isotropic. The other tendency results from synaeretic shrinkage of clusters. Because the intensity of both microscopic mechanisms are mineral and contaminant dependent, the coefficient β is contaminant and soil specific. The third term on the right-hand side is the plastic strain rate. Plastic potential function is assumed to be identical to the yield function, $f(\sigma'_{kl}, c)$. The plastic multiplier $\dot{\Lambda}$ is assumed to be dependent on stress and concentration rates.

The size of yield surface (taken as elipse, Reference 13), or in other words the elastic domain is also assumed to depend on the contaminant mass concentration

$$f = \left(\frac{2p'}{p'_c(\varepsilon_v^{\mathrm{pl}}, c)} - 1\right)^2 + \left(\frac{2q}{M(c)p'_c(\varepsilon_v^{\mathrm{pl}}, c)}\right)^2 - 1 = 0 \tag{3}$$

where p' is the mean principle effective stress, q is the second stress deviator invariant, equal to the principal stress difference in the case of axial symmetry, $\varepsilon_v^{\mathrm{pl}}$ is the plastic volumetric strain, M is the critical state coefficient related to the internal friction angle ϕ', through the relationship $M = 6\sin\phi'/(3 - \sin\phi')$. Internal friction angle, following the indications of Olson and Mesri[14] is postulated to be a function of mass concentration of the contaminant, and thus the critical state coefficient varies with concentration (Figure 1).

The apparent maximum preconsolidation isotropic stress p'_c for a single permeant is expected to shrink with decreasing dielectric constant, increasing ionic concentration, valency and temperature of the pore solution. Since all these properties of the solution vary with the contaminant

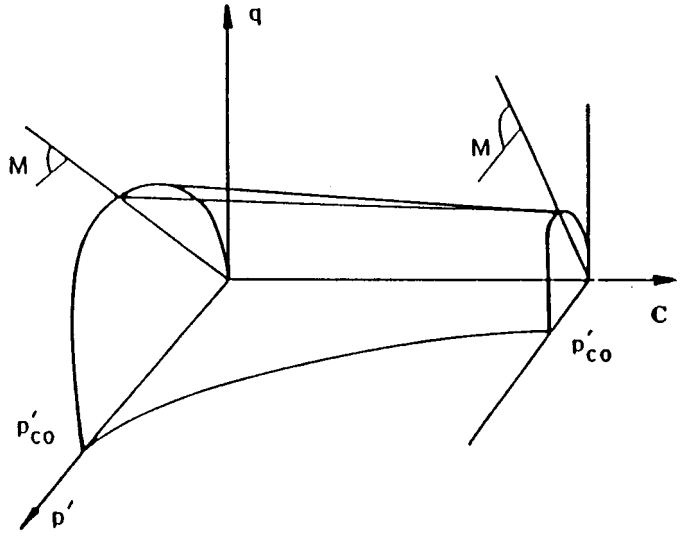

Figure 1. Representation of chemical softening of yield locus in q, p', and concentration space

concentration, the apparent maximum preconsolidation isotropic stress p'_c is proposed in a process of a monotonically increasing concentration at constant effective stress to be a phenomenological function of mass concentration. A two-fold dependence of p'_c on concentration is postulated as follows:

$$p'_c = p'_{c0} \exp\left(\frac{1 + e_0}{\lambda(c) - \kappa(c)} \varepsilon_v^{\mathrm{pl}}\right) S(c) \tag{4}$$

where λ and κ are, respectively, elastoplastic and elastic bulk moduli. Their dependence on permeant chemistry has been suggested by the observations of Fernandez and Quigley[6] on the clay skeleton decreased deformability induced by chemical damage, and by the chemical consolidation tests of Sridhran and Venkatappa Rao.[15] Note that the decrease in λ and κ (stiffening of clay) with increasing c, implies an increase of the size of the yield surface. However, the elastic domain observed was decreasing with increasing c, both for pure clay, for which plastic volumetric strain was zero, as well as in plastically pre-deformed clay, with $\varepsilon_v^{\mathrm{pl}} \neq 0$, as discussed by Hueckel.[16] Thus, an additional mechanism controlling the size of the yield surface is introduced, through the scalar multiplier $S(c)$ referred to as the chemical softening function, to reproduce the shrinking of the yield surface, even in the case of a pronounced decrease in the compliance moduli.

In the case of an abritrary process, the apparent maximum preconsolidation isotropic stress p'_c is obtained by integrating the part dependent on concentration and plastic strain rates separately

$$\ln\left(\frac{p'_c}{p'_{c0}}\right) = \int \left(\frac{(1 + e_0) S(c)}{\lambda(c) - \kappa(c)}\right) \dot{\varepsilon}_v^{\mathrm{pl}} + \int \left[\left(\frac{1 + e_0}{\lambda(c) - \kappa(c)} \varepsilon_v^{\mathrm{pl}}\right) \frac{\partial S}{\partial c} - \frac{(1 + e_0) \varepsilon_v^{\mathrm{pl}} S(c)}{[\lambda(c) - \kappa(c)]^2} \left(\frac{\partial \lambda}{\partial c} - \frac{\partial \kappa}{\partial c}\right) \right] \dot{c} \tag{5}$$

Although it needs to be confirmed experimentally for more permeants, it is expected that as a result of the superposition of chemical softening and chemical variability of the moduli λ and κ, the yielded surface shrinks, i.e. $\partial f / \partial c > 0$ for any c, $0 \leqslant c \leqslant 1$.

Plastic multiplier $\dot{\Lambda}$ is obtained analogously as in Prager's[17] thermo-plasticity theory from the consistency equation, assuming that during plastic strain in chemically active conditions, i.e. for $\dot{c} \neq 0$, the rates of effective stress, mass concentration and plastic strain are such that the yield function and its rate are always equal to zero

$$\dot{f} = \frac{\partial f}{\partial \sigma'_{ij}} \dot{\sigma}'_{ij} + \frac{\partial f}{\partial \varepsilon_v^{\mathrm{pl}}} \dot{\varepsilon}_v^{\mathrm{pl}} + \frac{\partial f}{\partial c} \dot{c} = 0. \tag{6}$$

Thus plastic multiplier $\dot{\Lambda}$ becomes

$$\dot{\Lambda} = \frac{1}{H} \left(\frac{\partial f}{\partial \sigma'_{ij}} \dot{\sigma}'_{ij} + \frac{\partial f}{dc} \dot{c} \right) \tag{7}$$

whereas the plastic strain hardening modulus H is

$$H = -\frac{\partial f}{\partial \varepsilon_v^{\mathrm{pl}}} \frac{\partial f}{\partial p'} \tag{8}$$

Thus, the constitutive law (2) can be rewritten by separating deviatoric and volumetric strains as functions of mechanical and chemical solicitation rates

$$\dot{\varepsilon} = \mathbf{D}\,\dot{\sigma} + \mathbf{C}\dot{c} \tag{9}$$

or

$$\begin{Bmatrix} \dot{\varepsilon}_v \\ \dot{\varepsilon}_q \end{Bmatrix} = \begin{bmatrix} D_{vp}^{\mathrm{el}} + D_{vp}^{\mathrm{pl}} & D_{vq}^{\mathrm{pl}} \\ D_{vq}^{\mathrm{pl}} & D_{qq}^{\mathrm{el}} + D_{qq}^{\mathrm{pl}} \end{bmatrix} \begin{Bmatrix} \dot{p}' \\ \dot{q} \end{Bmatrix} + \begin{Bmatrix} C_v^{\mathrm{el}} + C_v^{\mathrm{pl}} \\ C_q \end{Bmatrix} \dot{c}$$

where the elements of the constitutive matrix $\mathbf{D}$ and constitutive vector $\mathbf{C}$ are as follows:

$$D_{vp}^{\mathrm{el}} = \frac{\kappa}{1 + e_0} \frac{1}{p'}; \quad D_{vp}^{\mathrm{el}} = \frac{1}{H} \frac{\partial f}{\partial p'} \frac{\partial f}{\partial p'} \tag{10}$$

$$D_{vq}^{\mathrm{pl}} = \frac{1}{H} \frac{\partial f}{\partial q'} \frac{\partial f}{\partial q'}; \qquad D_{qq}^{\mathrm{el}} = \frac{1}{3\mathrm{G}}; \qquad D_{qq}^{\mathrm{pl}} = \frac{1}{H} \frac{\partial f}{\partial q} \frac{\partial f}{\partial q}; \tag{11}$$

$$C_v^{\mathrm{el}} = -\beta; \qquad C_v^{\mathrm{pl}} = \frac{1}{H} \frac{\partial f}{\partial c} \frac{\partial f}{\partial p'}; \quad C_q = \frac{1}{H} \frac{\partial f}{\partial c} \frac{\partial f}{\partial q} \tag{12}$$

The chemo-plastic loading and chemo-elastic unloading criteria result from equation (7) as follows. For chemo-elastic unloading:

$$f < 0 \quad \text{or} \quad f = 0 \quad \text{and} \quad \frac{\partial f}{d\sigma'_{ij}} \dot{\sigma}'_{ij} + \frac{\partial f}{dc} \dot{c} < 0 \tag{13}$$

For chemo-plastic loading, for positive hardening modulus

$$H > 0, \quad f = 0 \quad \text{and} \quad \frac{\partial f}{d\sigma'_{ij}} \dot{\sigma}'_{ij} + \frac{\partial f}{dc} \dot{c} > 0 \tag{14}$$

whereas for the negative hardening modulus

$$H < 0, \quad f = 0 \quad \text{and} \quad \frac{\partial f}{d\sigma'_{ij}} \dot{\sigma}'_{ij} + \frac{\partial f}{dc} \dot{c} < 0 \tag{15}$$

The last inequality in (15) implies a stronger restriction on stress rates in comparison to the iso-chemical case. In particular, in the strain softening range ($H < 0$) the range of statically admissible stress paths is substantially reduced. Inverse relationships, i.e. defining stress rate in response to strain rate and concentration rate may be obtained in a way analogous to that presented for thermo-plastic models for clays.[18]

It is interesting to analyze a particular case of purely chemical loading, i.e. at a constant effective stress, $\sigma'_{ij} = \text{const.}$, at yield, i.e. at $f = 0$, and $\dot{f} = 0$, for an increasing concentration, $\dot{c} > 0$, and thus for $(df/\partial c)\dot{c} > 0$. In such a case, it is seen from the consistency equation (6) that there is a continuous plastic strain hardening to compensate chemical softening. In such a case the plastic strain rate becomes

$$\dot{\varepsilon}^{\text{pl}}_{ij} = \frac{1}{H}\frac{\partial f}{\partial \sigma'_{ij}}\frac{\partial f}{\partial c}\dot{c} \tag{16}$$

It is worth noting that the above flow rule implies the generation of deviatoric plastic strain rates, for all stress states that have a non-zero deviatoric stress component as defined by the normality rule. An alternative chemically induced non-associativity analogous to the thermally originated one is discussed by Hueckel and Borsetto.[18]

INTERPRETATION OF CHEMICAL CONSOLIDATION IN THE PERMEABILITY TESTS WITH ORGANIC CONTAMINANTS

Fernandez and Quigley,[5,6] have investigated permeation with dioxane and ethanol of Sarnia clay and the effect on its hydraulic conductivity, with or without the presence of external effective stress. They have also studied the effect of the application of load after comlpetion of permeation. A summary of data is reproduced in Appendix and the data most important for this exercise, are represented by the cartoons in Figures 2 and 3. Only two cases are presented in these figures: the case of no externally imposed effective stress and that of an externally imposed vertical effective stress of 160 kPa. It must be emphasized that the actual effective stress is a sum of the externally imposed stress and of effective stress arising in response to the integrated seepage body forces. A maximum (bottom) value of these forces, $J_{\max}$ is given in the figures. The experiments of Fernandez and Quigley,[5,6] were conducted in a rigid wall permeameter, and the specimens were water-compacted vertically in a mold, and when loaded, they were subjected to K_0 stress state. A constant specific discharge flow pump was used. Thus, an increase in hydraulic conductivity was measured as a decrease in pore fluid pressure gradient. The elemental seepage stress is proportional to flow velocity (imposed as constant) and inversely proportional to permeability. Assuming that permeability is a function of contaminant concentration, and knowing that pore pressure was measured at a constant concentration across sepcimen, it is inferred that so was the seepage stress. Thus, the effective stress part resulting from the integrated seepage body stress and producing seepage consolidation is (theoretically) linearly distributed along the height of the specimen. Effect of change in viscosity during fluid substitution was included in data elaboration. Vertical settlements of the specimens which are visualized are total settlements for initial reference water followed by pure leachate, pure contaminant or contaminant-leachate mixture. All data refer to stationary states, that is to the situation after several pore volumes of the contaminated leachate have passed the specimen, yielding constant effluent mass concentrations.

Analysing Figures 2 and 3 it should be first noted that the maximum seepage stress induced by the imposed flow at no externally imposed stress is quite high for pure water (0 per cent solution)

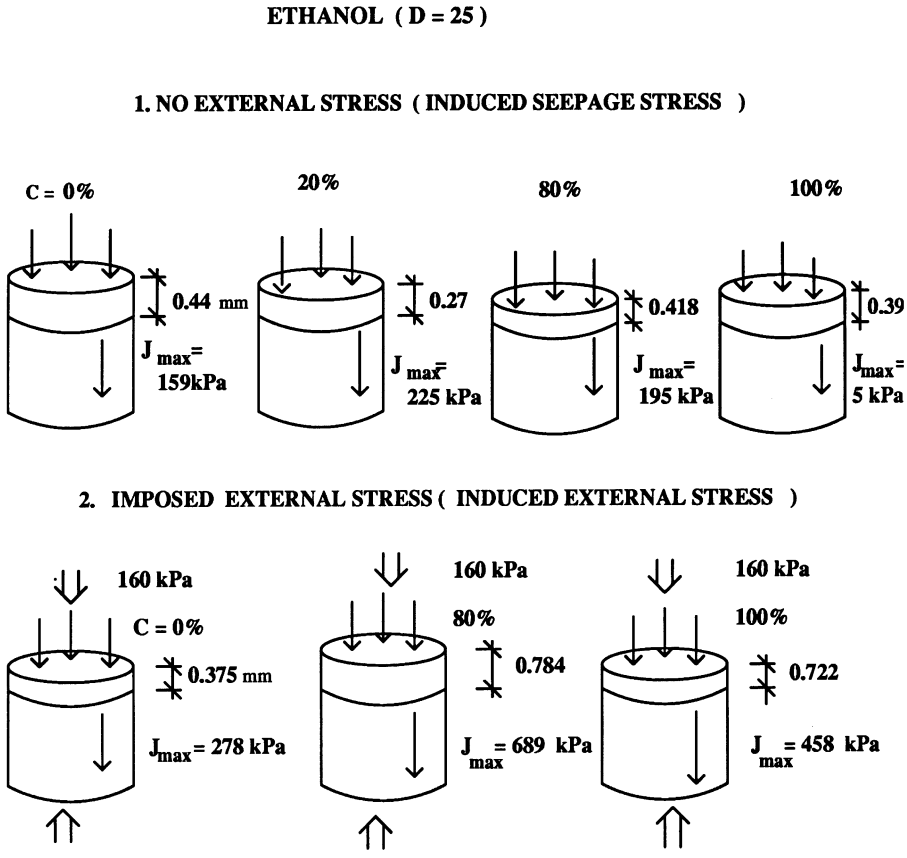

Figure 2. Cartoons showing the shortening of clay specimen and maximum seepage force due to flow of ethanol (dielectric constant $D = 25$) with different concentrations at (i) zero and (ii) an imposed external stress of 160 kPa (from the experiment of Quigley and Fernandez[6]; see also Table I in Appendix)

reaching 159 kPa and yielding a notable settlement of 0.44 mm of a 20 mm initial height specimen. However, during the flow of each of the contaminants, the settlements were lower for 20–80 per cent of mass concentration, even if the seepage forces were higher. They were further reduced for 100 per cent contaminated effluent when the seepage forces have drastically decreased. These observations suggest an important swelling deformation taking place during permeation, even for 20 per cent contamination. No such swelling is observed during permeation of the specimens preloaded with 160 kPa. Instead, a visible consolidation occurs during permeation already at 40 per cent of concentration. Clearly, a part of this consolidation may be attributed to the increase in seepage forces. However, comparing the consolidation data for intermediate imposed stress (Table I and II in Appendix, not reported in Figures 2 and 3, see Reference 6) one may realize that the additional consolidation occurs often at decreasing seepage forces. This consolidation cannot have other than a chemical origin.

We may now analyse the above data in the framework of the presented model for selected cases. The determination of the initial yield surface characterizing the material after compaction is the first step in the analysis. On the basis of an indirect estimation of stress–strain curve of static settlements at $c = 0$ (see paragraphs below, Fig. 8) the maximum apparent precompression

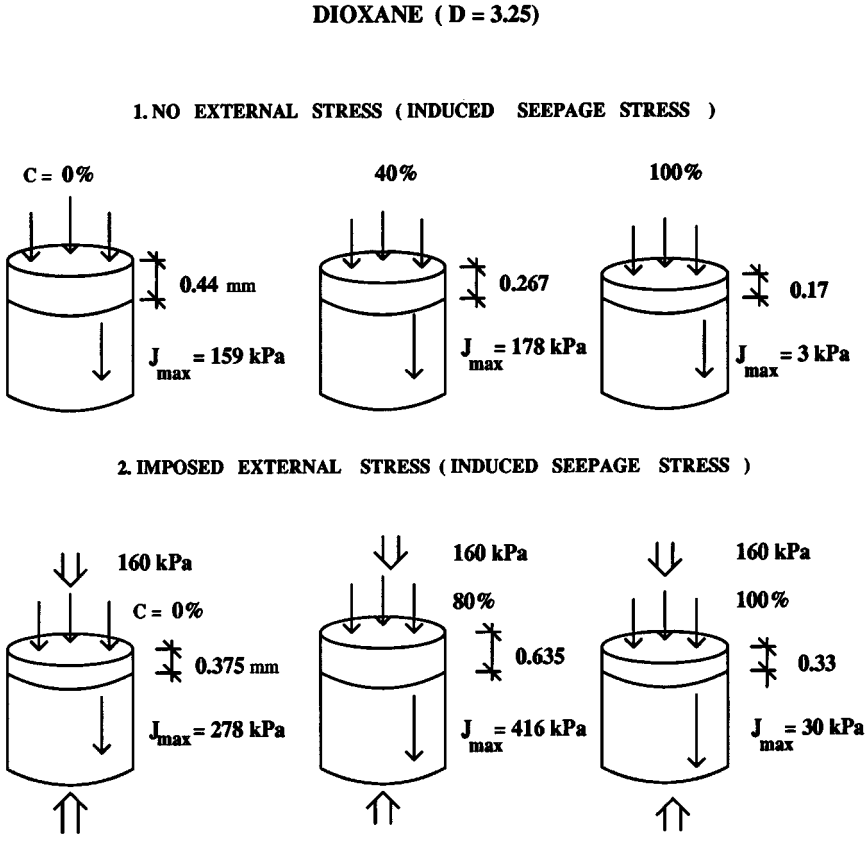

Figure 3. Cartoons showing the shortening of clay specimen and maximum seepage force due to flow of dioxane (dielectric constant $D = 3{\cdot}25$) with different concentrations at (i) zero and (ii) an imposed external stress of 160 kPa (from the experiment of Quigley and Fernandez[6]; see also Table II in Appendix)

vertical stress [point A in Figure 4(a)] reached in the compaction process has been estimated for 38·0 kPa. The term 'apparent' precompression stress is used because of the technique of dynamic compaction, which suggests a dubious meaning to the actual load on the specimen. Second, the consolidation settlement caused by the seepage forces must be determined to evaluate the strain due to chemical consolidation. During flow of water in the absence of any imposed external stress, there is actually a plastic loading due to relatively high seepage forces [A–B in Figure 4(a)] and a consequent plastic consolidation. At $c = 0$, the effective stress due to seepage forces at mid-height of the specimen equals 79·5 kPa, which is about two times the initial apparent precompression vertical stress. Thus, at least the lower half of the specimen is in the plastic state. This is confirmed by the value of the seepage settlement, which corresponds to the plastic range of the stress–strain curve (Fig. 8).

As for the mechanical response of clay to the flow of a contaminant, it consists, as far as the yield surface is concerned, of an interplay of strain hardening due to seepage consolidation and chemical softening at high concentration. As for strains, these consist in seepage consolidation, chemical swelling, as well as chemo-plastic consolidation. The latter one is activated depending on the position of the effective stress versus the current yield surface. During the test at zero

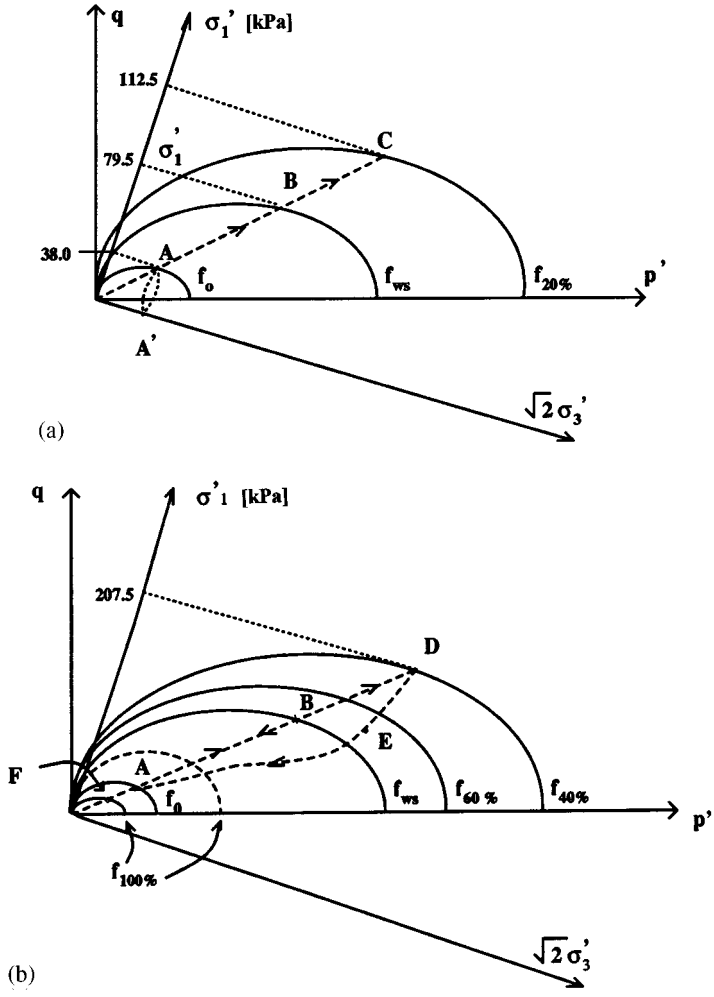

Figure 4. (a) Evolution of the yield surface corresponding to consequtive flow of water and 20 per cent ethanol at a constant specific discharge: f_0—yield surface after compaction; f_{ws}—yield surface during forced water flow: $f_{20\%}$—yield surface during forced flow of 20 per cent ethanol solution. A A′ A B C is the corresponding uniaxial strain compression effective stress path. (b) Evolution of the yield surface corresponding to the sequential flow of water and 100 per cent ethanol at a constant specific discharge: f_0—yield surface after compaction; f_{ws}—yield surface during forced water flow; $f_{40\%}$—the hypothetical largest yield surface during forced flow of 40 per cent ethanol solution; $f_{60\%}$—a chemicaly reduced yield surface during forced flow of 60 per cent ethanol solution; $f_{100\%}$—two hypothetical smallest, chemicaly reduced yield surface positions due to concomitant chemical softening and plastic strain hardening during forced flow of 100 per cent ethanol solution. For simplicity the possible effect of the increase of M is not shown. A B D E F is a corresponding uniaxial effective stress path. Note that point E is not at the yield surface, and thus corresponds to a chemo-elastic unloading stress path

external stress, with the permeation of 20 per cent ethanol, an increase in effective stress (point C) due to seepage forces resulting presumably from a decrease of permeability as a result of an increase of viscosity of the pore solution and a further expansion of the yield surface, is expected (Figure 4(a)). Nevertheless, the observed seepage settlement is lower than during pure water flow. This is attributed to the domination of chemical reversible strain. Note that, at this level of

concentration, no significant effect on hydraulic conductivity is yet seen, and thus no visible chemical softening may be hypothesized. Thus, the deformation at low concentration is chemo-elastic and plastic, but not chemo-plastic.

At high concentration of ethanol, e.g. 100 per cent, the mechanisms involved are different. Assuming that the growth of contamination in the whole specimen is not instantaneous (or that the transport mechanism is advection accompanied by diffusion and dispersion, and thus a concentration at the center of the specimen has a finite rate), the effect of gradual increase of c needs to be considered. Thus, the first phase of the process at low concentrations is identical to the one described above. However, when c grows above 40 per cent, one observes an unloading, D–E–F, of the seepage forces needed to push the permeant through clay, with respect to the situation generated during water flow. At the same time, the yield surface shrinking (chemical softening) due to contamination becomes significant. The deformation of clay may now be either elastic or plastic, depending on which of the above two processes has a higher rate. If the stress rate during unloading is higher than the rate of chemical softening, then the stress point is all the time inside the yield surface, and the process is chemo-elastic. If on the contrary, the rate of shrinking of the yield surface is higher than the corresponding effective stress rate, at some point, the stress point and the yield surface can meet and the process becomes chemo-elasto-plastic, states E–F, Figure 4(b). A compactive plastic component of strain then adds to the expansive chemical strain and to elastic expansion strain due to unloading of seepage stress. The plastic strain will induce strain hardening and the resulting rate of shrinking may be lower. At 100 per cent contamination by ethanol, the high value of settlement, only slightly less than that during water flow, may indicate some amount of chemical consolidation superposed on swelling due to seepage stress unloading. The final position of the yield surface cannot be determined with certainty, without reloading performed. It must be also emphasized that the analysis performed here is approximate in the sense that it is assumed that the stress path is dominated by the imposed stress changes and not excessively affected by the presence of the chemical strain, which could deviate the stress path from the K_0 conditions.

For dioxane, at low contamination, both the increase in seepage forces and settlements are generally lower than in ethanol. For both 85 and 100 per cent of dioxane contamination, the seepage stresses are drastically reduced, and both the seepage stresses and settlements are visibly lower than in ethanol. Most probably the chemical softening does not progress too far. It seems that the chemical softening due to dioxane contamination is less significant than for ethanol. Consequently, the final yield surface at 100 per cent contamination for dioxane seems to be larger than for ethanol.

When an external load is imposed prior to contamination, as for ethanol at 160 kPa case, see Figure 5(a), the situation does not change from the qualitative point of view, with respect to the previous one. In fact, the stress generated by the seepage forces is of the same order as the effective stress due to the imposed load. The settlements due to seepage of pure water are smaller (0·375 mm) than in the case of no external load (0·446 mm), presumably due to pre-stress compaction. In the tests with ethanol the seepage settlements (about 0·7 mm) were all clearly higher than in the water case (0·375 mm) and very close to one another for all pre-stress values, and for all concentrations, see Table I. It is imaginable that the plastic process has been initiated by the water seepage stress, at C, continued during contamination, D, as seepage forces increased due to the increase of the permeant viscosity. At 100 per cent ethanol concentration, when a slight drop in seepage forces was seen, the strain hardening due to chemical consolidation manifested as increased settlements must have been high enough to prevail over the yield surface shrinking due to chemical softening. As a result, the final yield surface, E, remained quite large.

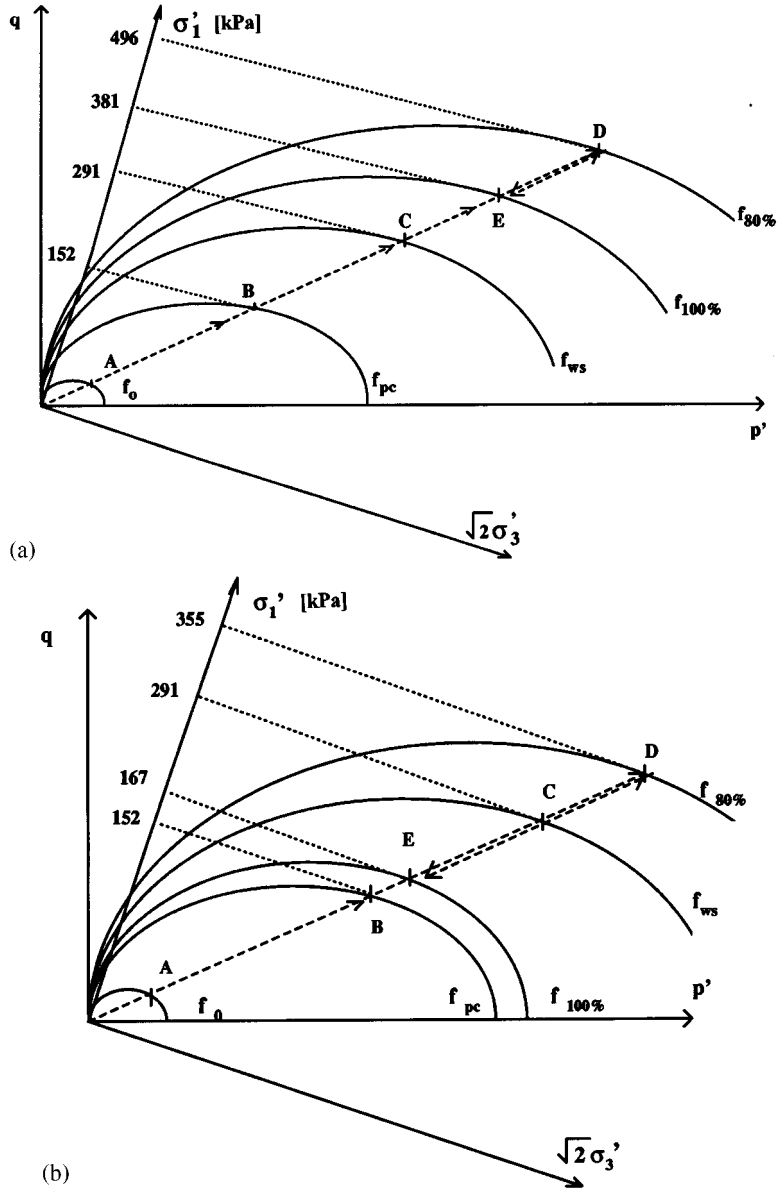

Figure 5. (a) Evolution of the yield surface corresponding to the pre-loading to 152 kPa and consequtive flow of water and 100 per cent ethanol at a constant specific discharge: f_0—yield surface after compaction; f_{pc}—yield surface after pre-loading; f_{ws}—yield surface during forced water flow; $f_{80\%}$—the hypothetical largest yield surface during forced flow of 80 per cent ethanol solution; $f_{100\%}$—the chemicaly reduced yield surface subjected to concomitant chemical softening and plastic strain hardening during forced flow of 100 per cent ethanol solution. For simplicity the possible effect of the increase of M is not shown. ABCDE is the a corresponding uniaxial effective stress path. Point B corresponds to the externally imposed stress. Note that during unloading started at D, i.e. at 80 per cent the overall effective stress did not decrease to the value at B. The difference between points E and B corresponds to the seepage stress at 100 per cent contamination. (b) Evolution of the yield surface corresponding to pre-loading to 152 kPa and consequtive flow of water and 100 per cent dioxane at a constant specific discharge: f_0—yield surface after compaction; f_{pc}—yield surface after pre-loading; f_{ws}—yield surface during forced flow; $f_{80\%}$—the hypothetical largest yield surface during forced flow of 80 per cent dioxane solution; $f_{100\%}$—the chemicaly reduced yield surface subjected to concomitant chemical softening and plastic strain hardening during forced flow of 100 per cent dioxane solution. ABCDE is the corresponding uniaxial effective stress path. Point B corresponds to the externally imposed stress. Note that during unloading started at D, i.e. at 80 per cent the overall effective stress decrease to the value at E, relatively much more than in the corresponding circumstances in ethanol, presumably due to much higher reduction in seepage stress. The difference between points E and B corresponds to the seepage stress at 100 per cent contamination. Note how it compares to that in ethanol

Clearly, it is realized that since the seepage stress varies linearly (theoretically) along the height of the specimen, the effective stress distribution is trapezoidal, with its maximum at the specimen bottom. In the above analysis the effective stress is assumed as uniformly distributed and equal to its actual value in the upper part of the specimen. Such an assumption induces an overestimation of stress in the upper part of the specimen and an underestimation in its lower part. In particular, the former approximation may lead to a premature prediction of yielding and as a consequence to an overestimation of plastic strain in the upper part and its underestimation in the lower part of the specimen. It is expected that by taking a mean value the error is minimized. A low flow pump discharge is therefore recommended for such experiments to reduce the seepage forces.

For dioxane, Figure 5(b), the seepage forces were usually lower than those for ethanol and there was a drastic seepage force decrease (and permeability increase) at 100 per cent concentration for all loads. The corresponding amounts of settlement were also less than in the case of ethanol. For lower concentrations this can be explained by an almost 50 per cent lower viscosity change in the permeant mixed with dioxane. For 100 per cent concentration, evidently the chemical softening was less intense ('slower') than the observed pronounced seepage force drop, and most of the contamination process was chemo-elastic, while plasticity entered the picture for a fraction of the process, at intermediate concentrations.

Finally, let us consider the tests with a post-contamination compression.[6] These tests were performed to examine the possibility of healing the chemically induced damage to hydraulic conductivity, by applying an effective stress to clay not before, but after the flow of contaminant. As visible from Figure 6(a) and (b), the operation was successful with a modest load in the case of 100 per cent ethanol and much less for 100 per cent dioxane. This seems to be related to the differences in settlement during the post-contamination compression which in the case of the ethanol permeated specimen was almost 50 per cent larger than that with dioxane.

The differences can be explained by the presented model in the following way. First, it should be realized that the application of the effective stress before and after contamination has a completely different meaning in terms of plasticity theory. In the former case the effective stress during early contaminant flow was increasing due to seepage stress increase controlled by viscosity, while at 100 per cent it decreased. Thus, the deformation causing the 'healing' of permeability during pre-contamination mechanical loading was induced by the *concentration* increase. In the post-contamination loading case the 'healing' deformation is due to *stress* increase at zero concentration rate. It seems, from the previous considerations, that the sensitivity of the yield surface to the two liquids is different and ethanol induces more advanced chemical softening, but its flow is counteracted by higher seepage forces than for dioxane. Eventually, the elastic domain is smaller after the permeation with ethanol than in the case of dioxane, Figure 7.

The post-permeation straining of the specimen is purely mechanically driven, and the difference between the response of the two permeants may be attributed to the differences in the initial positions of yield surfaces and differences in the chemical dependence of elasto-plastic bulk modulus $\lambda = \lambda(c)$. It has been suggested by Fernandez and Quigley[6] that the overall compressibility decreases more significantly with dioxane, than with ethanol. It should be noted that seepage stress and consolidation are growing higher for ethanol than for dioxane as permeability drops. Experiments which would include both chemical and mechanical loading and unloading might help in a better understanding of the above process.

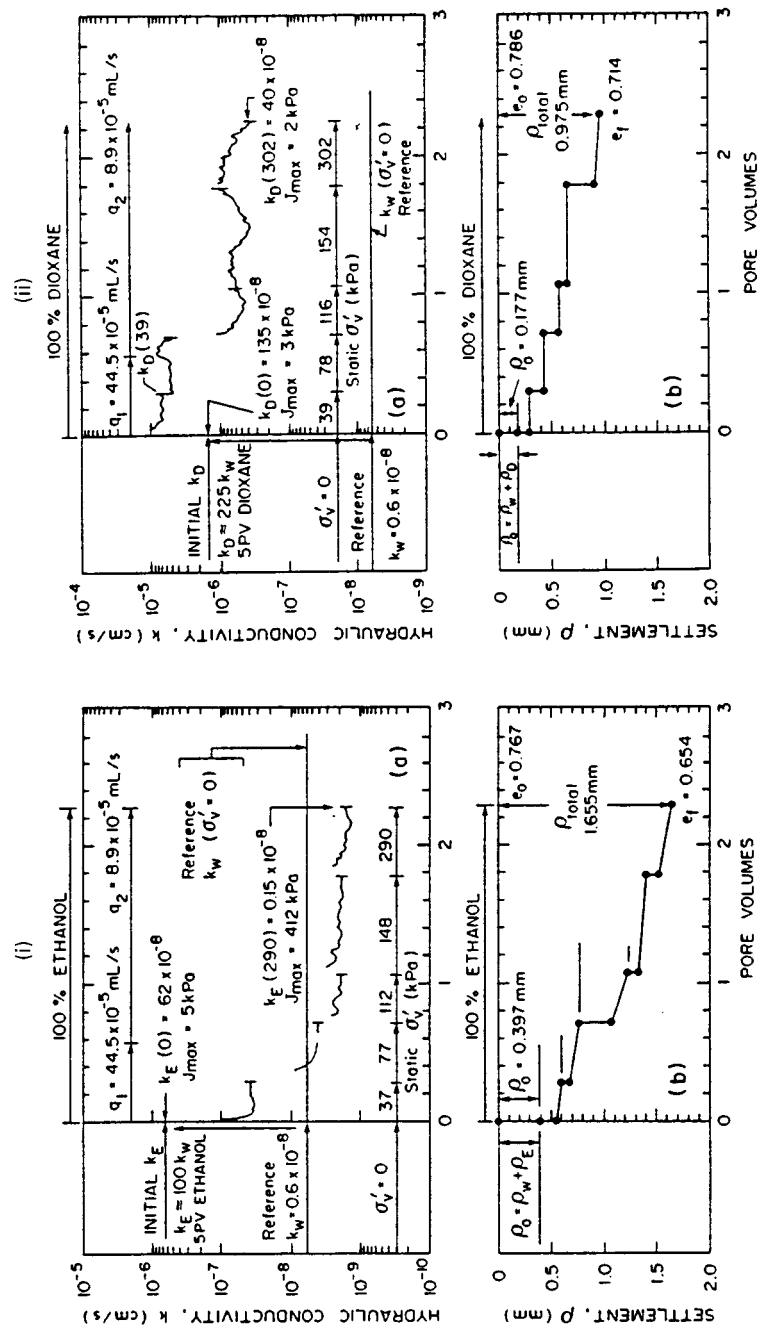

Figure 6. Healing the chemically induced damage to hydraulic conductivity, by post-contamination application of the effective stress to water-compacted clay: (i) in the case of 100 per cent ethanol, with the effective stress due to external load of 37, 77, 112, 148 and 290 kPa: (ii) flow of 100 per cent dioxane, with the effective stress due to external load of 39, 78, 116, 154 and 302 kPa: (a) hydraulic conductivity versus volume of permeated liquid in terms of pore volumes and (b) vertical settlement of 20 mm high specimen (from Reference 6)

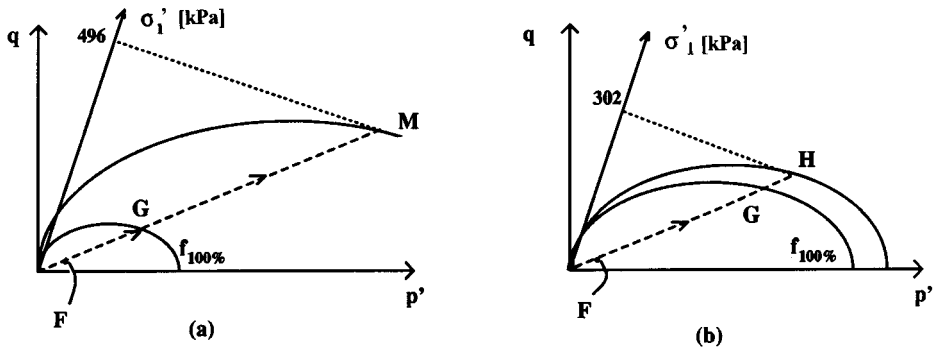

Figure 7. Post-damage loading for ethanol (a) and dioxane (b). The plastic portion is more extensive in ethanol than in dioxane because of differences in the terminal position of the yield limit after 100 per cent contamination. The actual effective stress on ethanol permeated specimen is higher than that resulting from the external loading due to increasing seepage stresses related to the decreasing permeability

DETERMINATION OF CHEMO-PLASTICITY PARAMETERS

This section is aimed at the calibration of the proposed model for the clay and contaminants used in experiments by Fernandez and Quigley.[6] To be able to calibrate the model, several simplifications need to be made, mainly because some data needed for the calibration were not available. First, it will be assumed that elasticity is contamination independent, second, that the chemical expansion function is stress independent, and third, that friction angle, or critical state coefficient is constant. As for the hardening bulk modulus, λ, it is assumed to be contamination independent in the first phase of our calculation, when we determine the chemical softening function. We shall investigate the actual variations of plastic modulus as a function of concentration at the end. Given the above assumptions, the functions to be determined in the first phase are: the chemical expansion function β and chemo-plastic softening function, $S(c)$, responsible for the chemically induced yield surface shrinking.

The chemical expansion function is best determined in an elastic stress state. To distinguish between elastic and elasto-plastic states the unloading criterion needs to be checked against the stress state $f(\sigma'_{ij}, c) < 0$. Because the lateral stress components are not known, an approximate criterion based on axial stress component only will be used. This is justified if the $K_{0\,(\mathrm{NC})}$ stress path during loading and different, $K_{0\,(\mathrm{OC})}$ stress path during unloading, do not differ substantially. The chemical expansion in the elastic range may be obtained as a difference between the total strain (experimentally measured) and mechanically induced, stress-dependent strain,

$$\varepsilon_v^{\mathrm{chel}}(c) = \varepsilon_v - \varepsilon_v^{\mathrm{el}}(p') \tag{17}$$

where the mechanically induced volumetric strain is

$$\varepsilon_v^{\mathrm{el}}(p') = \frac{\kappa}{1 + e_0} \ln \frac{p'}{p'_0} \tag{18}$$

To determine the elastic and plastic strains, an isochemical isotropic stress–volumetric strain curve is first determined from the experimental data assuming an elasto-plastic behaviour of clay (Figure 8). Strain for this diagram is obtained from the settlements of the specimen due to both the static vertical load and the seepage forces during flow of pure water. In the absence of the information about lateral stress, the ratio $\sigma'_h/\sigma'_v = K_0$ is evaluated on the basis of the plasticity

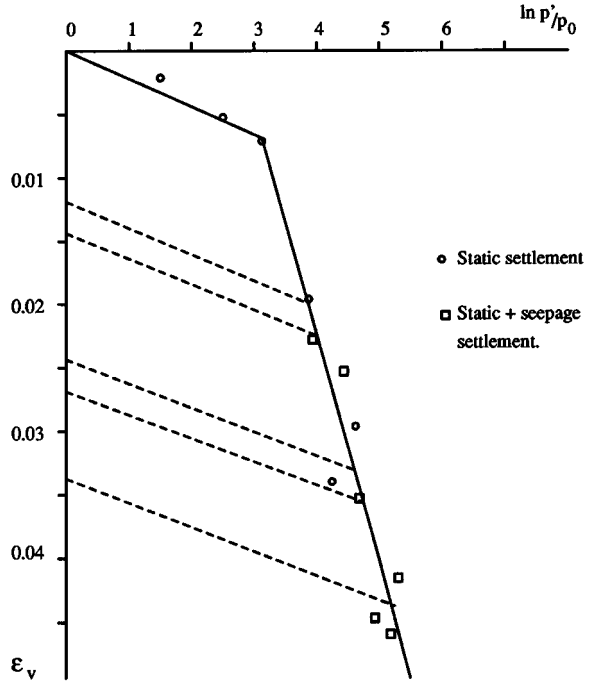

Figure 8. Logarithmic isotropic stress versus volumetric strain in 1-D (oedometric) compression reconstructed for Sarnia compacted clay from static (○) and water seepage induced (□) settlements measurements. The actual vertical stress has been esetimated as $\sigma'_v = 1.51p'$. The values p'_0 is 1 kPa

index, I_p, equal to 20·5 per cent, from the empirical relationship of Brooker and Ireland[24], as $K_0 = 0{\cdot}19 + 0{\cdot}233 \log I_p = 0{\cdot}49$. This relationship is applied for clay in non-contaminated state. It allows to determine the relationship between the vertical stress and isotropic effective stress $p' = 0{\cdot}66\sigma'_v$ for specimens in the state of normal consolidation. The maximum apparent preconsolidation isotropic stress p'_{co} can also be estimated, assuming the elliptic yield condition, equation (1), and for $K_0 = 0{\cdot}49$, it is $p'_{co} \approx \sigma'_{v0}$. The latter stress has been estimated using Casagrande technique as equal to $\sigma'_{v0} = 38$ kPa, corresponding to $p' = 25$ kPa. The logarithmic bulk modulus of elasticity (κ) was determined to be 0·00396. The elasto-plastic modulus (λ) obtained for this plot was found to be 0·0324.

Figures 9(a)–(c) present the values of total volumetric strain versus concentration for clay being permeated with a solution of ethanol, for different nominal external loads, elaborated on the basis of the experiments of Fernandez and Quigley.[6] Figures 10(a) and (b) show an analogous relationship for dioxane solutions. Total volumetric strain is equivalent to the settlement due to initial static consolidation under load in water, followed by the settlement due to flow of water and then of the contaminant. The values of the settlements are taken from Tables I and II (Appendix). The specimen height is 20 mm. Lateral strain is assumed to be zero, given the oedometric conditions.

Additionally, in Figures 9 and 10, the part of the volumetric strain is shown, which would arise from purely mechanical loads in the absence of any chemical effect. These purely mechanical loads include the vertical stress applied externally and stress in the specimen induced by the integrated seepage body forces. An average value is taken for the seepage stress equal to $J_{max}/2$.

The consequences of this assumption were discussed earlier. It should be noted that the strain at some states had been calculated including the history of loading and unloading to an elastic state, when the total stress during flow of contaminants were lower than those imposed during water flow. The difference between the measured strain and the mechanically induced strain is attributable to chemical effects.

It should be noted that the total (measured) strains in the ethanol permeated specimens at no nominal stress, are expansive at low concentration, then for intermediate concentrations, clay appears to be more consolidated, and finally at high concentrations it again becomes less consolidated. Some of these effects can be explained through variations in the seepage generated stresses, which increase between $c = 20$ and 40 per cent (viscosity induced permeability drop) and the drastically decrease near $c = 100$ per cent. The differences between the measured strains and the mechanically induced ones are considered in this model as those of chemical expansion, analogous to thermal expansion. They are indeed expansive for $c < 65$ per cent and are attributed

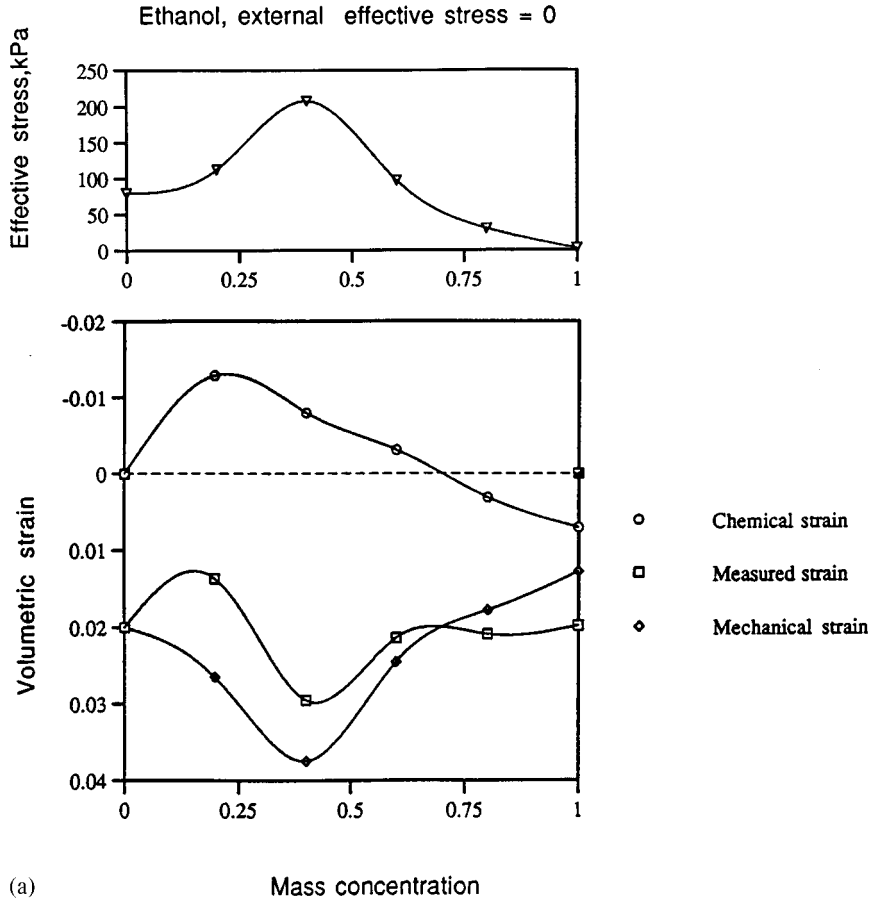

Figure 9. Ethanol permeated clay: effective stress (externally induced and due to seepage), measured (total) volumetric strain, calculated mechanical volumetric strain due to total effective stress (due to external and seepage load), and chemically induced volumetric strain, versus mass concentration c for different nominal external loads, as elaborated on the basis of the experiments of Fernandez and Quigley;[6] (a) at no externally induced effective stress, (b) at externally induced effective stress of 40 kPa; (c) at externally induced effective stress of 80 and 160 kPa

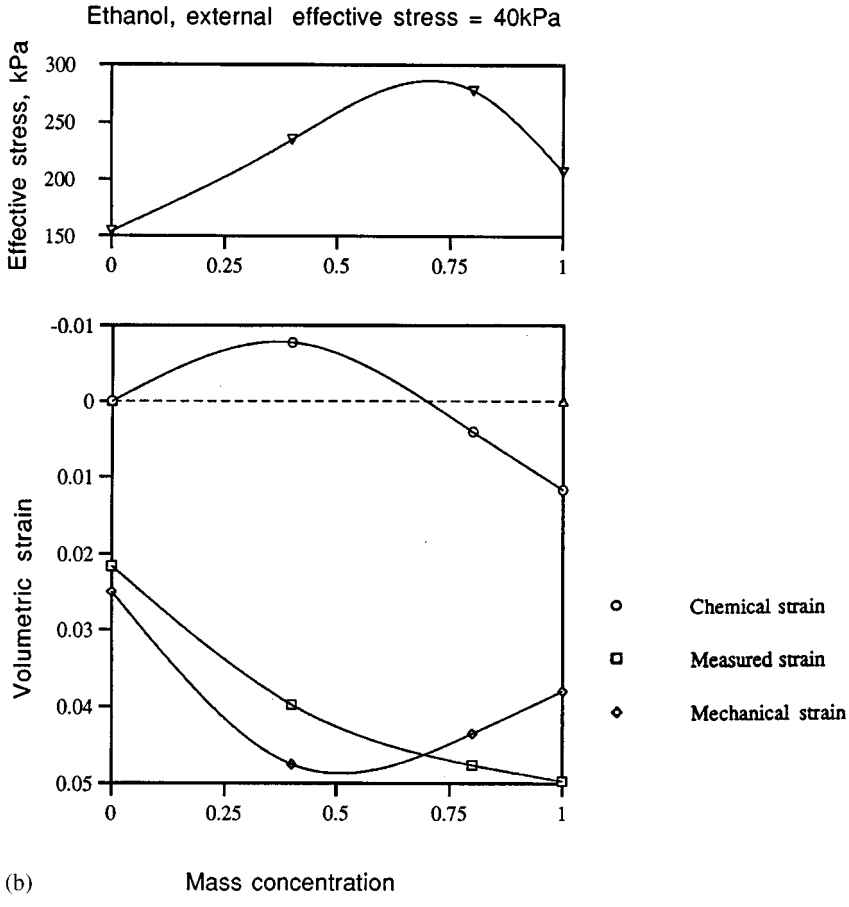

Figure 9. Continued

to the tendency to flocculate on the microscopic level. At higher concentrations, specifically for $c > 65$ per cent the strain difference becomes compressive which is attributed to chemo-plastic consolidation starting at, or slightly below $c = 65$ per cent, where their rates become compressive. Note that, on the microscopic level, the response to concentrated organics is a resultant of the volume changes due to often opposite changes in the mass of adsorbed water, and flocculation.[19] Although these observations were performed on Na-montmorillonite suspensions, and do not necessarily correspond quantitatively to the volume changes in compacted clays, the general tendencies are the same. Also, it must be emphasized that the net result depends on clay minerology. In the discussed Sarnia clay specimens the smectitic fraction was Ca-saturated and did not show fractures when contaminated nor any significant changes in pore distribution. Clays for which chemically induced fractures were reported were Na-montmorillonites[20] and presumably subjected to synaeretic shrinkage dominating over the expansion due to particle reorientation. Other reports on chemically induced fractures were not quantitative and did not specifically distinguish between Ca and Na clays.[3] Synaeretic shrinkage and cracking require a separate consideration related to a fracture criterion.

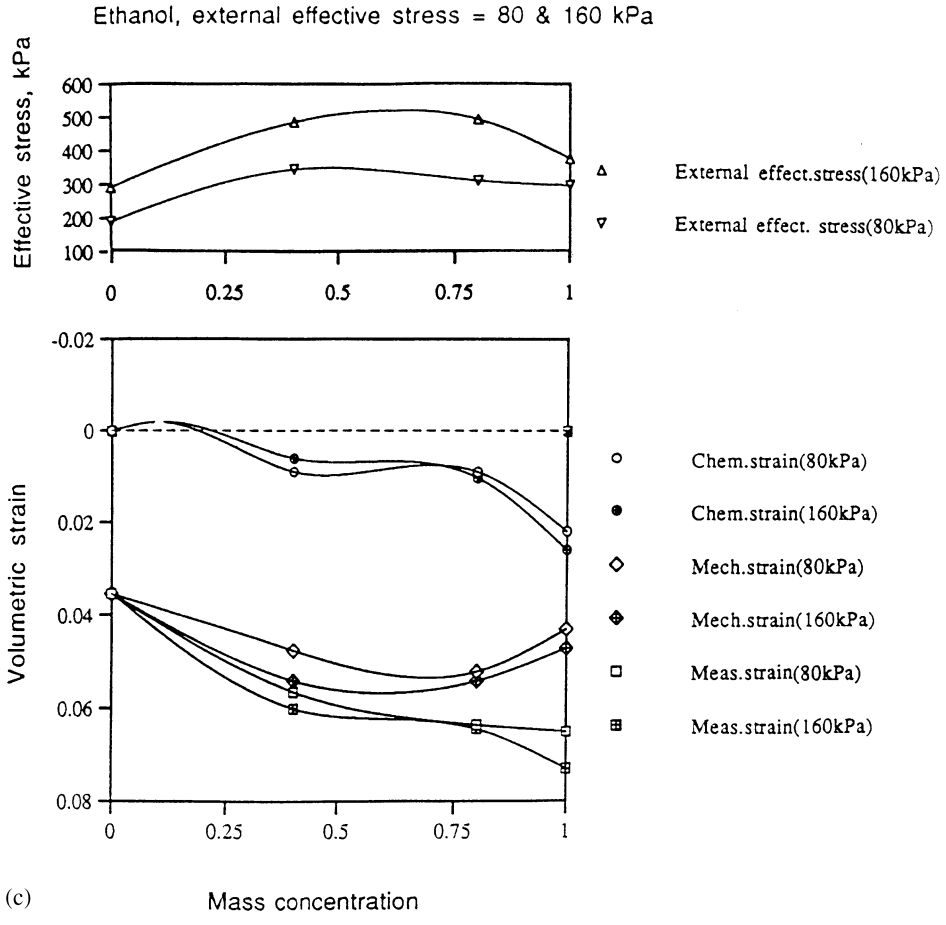

Figure 9. Continued

Unfortunately, for higher nominal external stresses of 40, 80 or 160 kPa there is no data for $c = 20$ per cent. However, for higher concentrations the measured compressive strain rate consistently monotonically grows with concentration.

For dioxane at no nominal external stress, the measured compressive strain at all concentrations is lower than during flow of water, and also lower than the strain attributable to mechanical loading. This yields the chemically induced strain difference expansive for all concentrations, and increasing with concentration up to $c = 70$ per cent. However, for $c = 85$ and 100 per cent the strain difference seems to be insensitive to concentration. For pre-compressed specimens, the total (measured) strain–concentration curves are quite different, especially at 100 per cent, and therefore the chemically induced strain difference is different from that in the specimens that were not pre-compressed. In particular, the chemical strain difference is compressive, and at 100 per cent becomes smaller than for lower c, or nearly zero.

In order to determine the chemo-elastic strain function, the evolution of the yield surface needs to be determined to make sure that the stress states considered are elastic. During permeation of clay with dioxane following the pure water flow at no external stress, such a state may arise at low

concentrations, due to a sight drop of mean seepage stresses from 159/2 kPa to 120/2 kPa and 127/2 kPa, at concentrations of 10 and 20 per cent, respectively, causing a slight unloading of effective stress, see Figure 10(a) (top). The measured strain rate accompanying this unloading is expansive and it is much higher than that expected as a result of elastic unloading, yielding the reduction of total compressive strain from 0·22 to 0·0195, see Figure 10(a) (bottom). We assume that the chemical softening until $c = 20$ per cent is not yet such as to visibly affect the yield surface. However, at $c = 40$ per cent the seepage stresses increase due to viscosity change of the permeant causes slight yielding and consequently we can consider as elastic only the states for $c < 40$ per cent. Thus, pure chemo-elastic strain is assumed to occur for $c < 40$ per cent. After a slight increase of effective stress at $c = 40$ per cent, the stress drop starts. Despite the drop in seepage stress and thus in effective stress the specimen swelling is arrested.

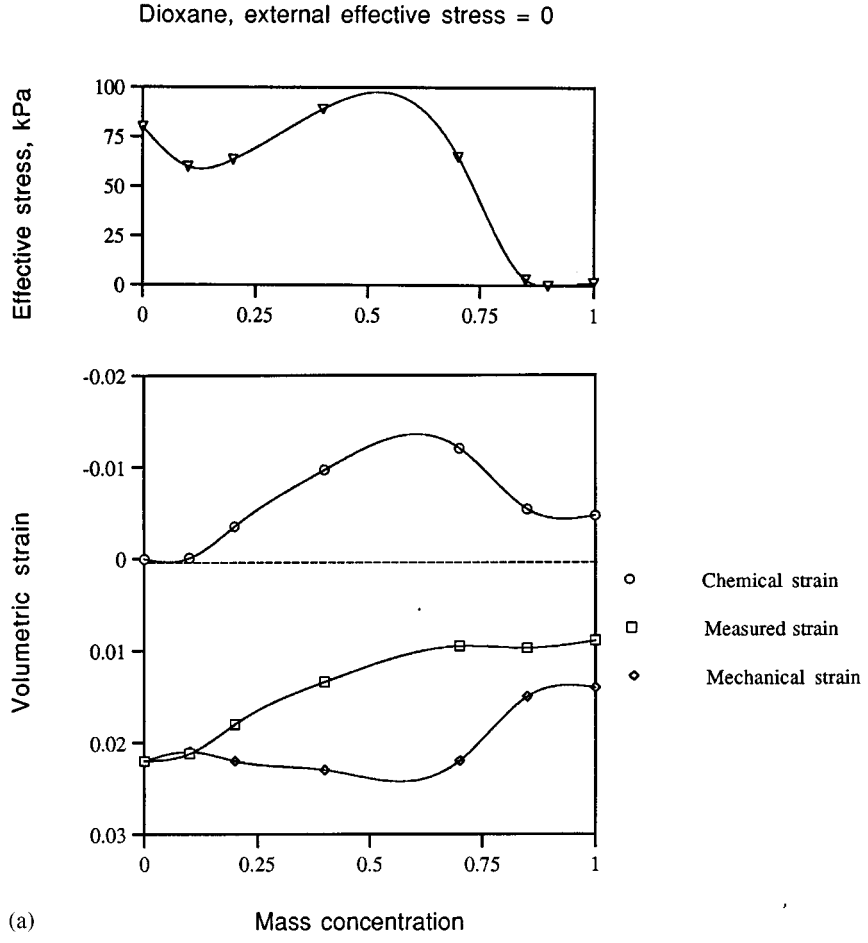

Figure 10. Dioxane permeated clay: effective stress (externally induced and due to seepage), measured (total) volumetric strain, calculated mechanical volumetric strain due to total effective stress (due to external and seepage load), and chemically induced volumetric strain, versus mass concentration c for different nominal external loads, as elaborated on the basis of the experiments of Fernandez and Quigley;[6] (a) at no externally induced effective stress, (b) at externally induced effective stress of 40, 80 and 160 kPa

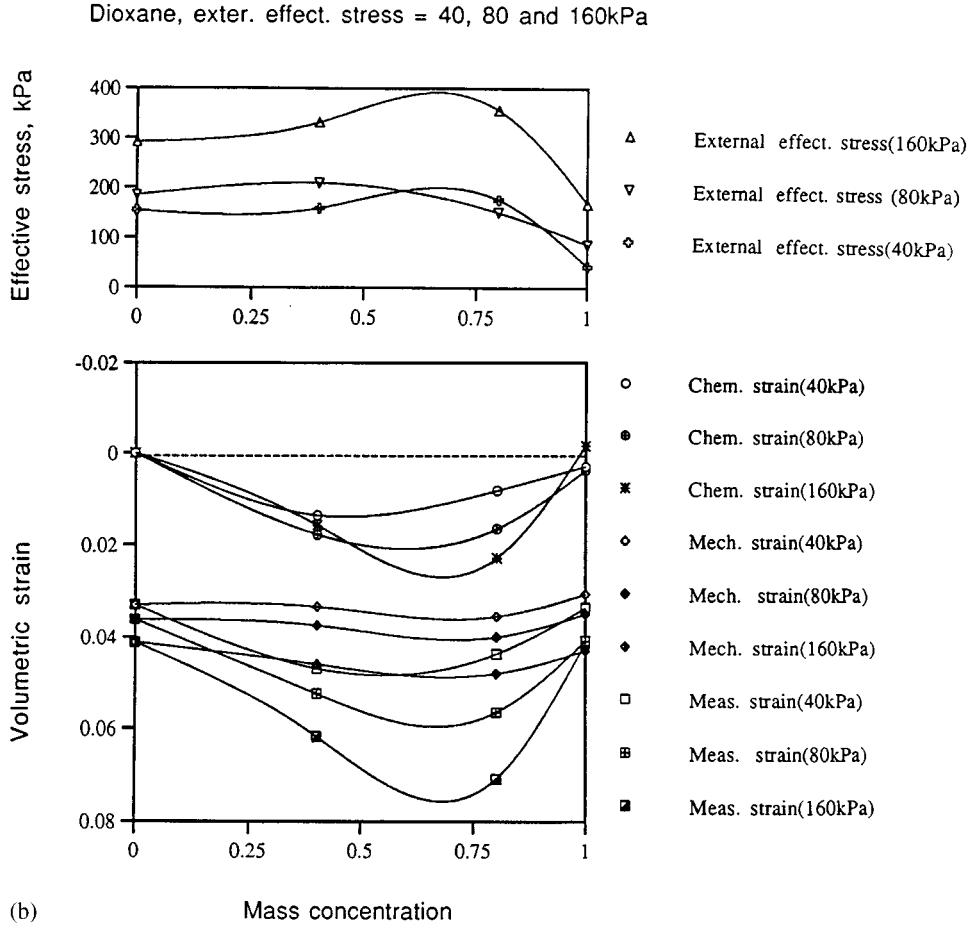

Figure 10. Continued

The presence of compressive strain difference rate for concentrations larger than about 60 per cent, despite effective stress unloading, prompted us to assume that the chemo-plastic consolidation has occurred. Furthermore, at concentrations between 85 and 100 per cent there is no further significant effective stress change, and thus no expected mechanical strain change, nor there is any significant change in the measured total strain. This suggests that at concentrations between 85 and 100 per cent there is no further chemo-plastic consolidation, to be attributed to a drop in effective stress faster than the chemical softening, causing an unloading. It also suggests that concentrations between 85 and 100 per cent do not produce any further chemo-elastic expansive strain. It is quite realistic to envisage a physical limit to the flocculation strain for purely geometrical and microstructural reasons. Given the above, the chemical strain from Figure 10(a) for $c = 10$, 20 and 40 per cent is extrapolated above $c = 40$ per cent as a non-linear function of concentration, reaching a horizontal asymptote at $c = 100$ per cent, as presented in Figure 11.

We additionally assume that the chemo-elastic strain function does no explicitly depend on the effective stress. It can clearly be suppressed by geometrical constraints producing compressive

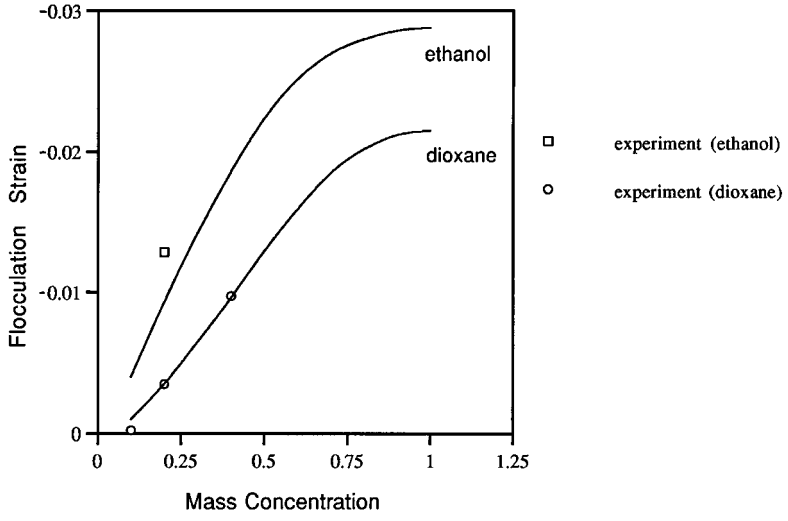

Figure 11. Chemo-elastic (flocculation) volumetric strain versus mass concentration. Experimental and extrapolated theoretical points for ethanol and dioxane permeation at no external stress

stress, in analogy to the stress produced by a constrained thermal expansion. Visibly, chemo-elastic strain requires further careful testing and analysis. For the current purpose, it is proposed to be represented as an exponential function of concentration in the form

$$\varepsilon_v^{\text{chel}} = F_0 \exp[\beta_0(1 - c + \ln c)] \tag{19}$$

where F_0 is the limiting chemo-elastic strain value, while β_0 is determined from the slope of the strain–concentration curve at the point $F_0/2$. Thus, the coefficient of rate of volumetric chemo-elastic expansion in equation (3) is

$$\beta = F_0\beta_0 \exp[\beta_0(1 - c + \ln c)]\left(\frac{1}{c} - 1\right) \text{ or } \beta = \beta_0 \varepsilon_v^{\text{chel}}\left(\frac{1}{c} - 1\right) \tag{20}$$

The value of the asymptotic strain for dioxane is assumed to be $F_{0d} = -0{\cdot}0215$, corresponding to the strain resulting from the linear relationship at $c = 80$ per cent, where the total strain levels off.

As for the chemo-elastic function in ethanol, it is seen from Figure 9(a) that right from the very low concentrations, the increasing seepage stresses are producing plastic loading during flow of the contaminant. However, the measured consolidation at $c = 20$ per cent is clearly lower than that during the pure water flow. Thus, the chemical strain difference is still expansive. We assume that this is not yet any significant chemical softening at $c = 20$ per cent and the entire chemical strain difference at this concentration is due to the tendency to flocculate. Unfortunately, this is the only chemo-elastic strain value at our disposal. Therefore, we shall make an assumption that the limiting value for the chemo-elastic strain in ethanol is $F_{0e} = -0{\cdot}029$, which is the value resulting from a linear dependence at $c = 60$ per cent, at which we observe a levelling off of the total strain curve, Figure 9(a).

The numerical values of the coefficients β_0 were found from the initial slope of the stress–concentration curves to be $\beta_{0e} = 2{\cdot}55$ for ethanol and $\beta_{0d} = 1{\cdot}32$ for dioxane. The experimental points and the numerical approximations are compared in Figure 11. Clearly, a more

rational procedure needs to be devised to determine the entire chemo-elastic strain curve, including its possible effective stress dependence. One possible technique would require performing a sufficient mechanical precompression prior to contamination to avoid the chemo-plastic consolidation at higher concentrations, when the yield surface pressumably shrinks to meet the effective stress point. Chemical unloadings (de-contamination) after each concentration step would be desirable to determine the chemo-plastic strain directly from experiment.

For the characterization of the chemical softening function $S(c)$, we shall consider stationary contamination processes in which $\dot{c} = 0$, but $c \neq 0$, at constant effective stress (including the seepage stress component), as those reached in the tests by Fernandez and Quigley.[5,6] For such states at yielding it is possible to employ the equation for the hardening/softening rule function. This function expresses an explicit relationship between volumetric plastic strain, concentration, the actually applied effective stress (seepage stress included), and the apparent preconsolidation isotropic stress p'_{c0}, which for $d\sigma'_{ij} = 0$ can be substituted by the known stress value.

$$\frac{p'_c/p'_{c0}}{\exp\{[(1+e_0)/(\lambda-\kappa)]\}\,\varepsilon_v^{pl}} = S(c) \tag{21}$$

To determine the chemo-plastic softening function $S(c)$, the value of the current size of the yield surface, p'_c, its initial value, p'_{c0}, the values of the two moduli, λ and κ, and the value of the plastic volumetric strain need to be known. The isochemical values of moduli λ and κ, are determined from Figure 8, since the moduli have been assumed as not affected by chemistry for this procedure. Depending on whether the state is considered as that of loading or unloading, the yield surface size may be estimated either from the current or from the maximum past externally imposed load and seepage stress data. The estimate of volumetric plastic strain for plastic flow states, is based on the additivity principle for small strains, which reads

$$\varepsilon_v^{chpl}(p', c) = \varepsilon_v - \varepsilon_v^{el}(p') - \varepsilon_v^{chel}(c) \tag{22}$$

The value of total volumetric strain ε_v, can be calculated from the vertical settlements measured directly in the experiment, and assuming, due to lack of data, that lateral strain components of all, i.e. plastic and elastic as well as chemo-elastic strain parts are zero independently. This assumption may be questioned, especially, for chemo-elastic expansion, if it is viewed as an isotropic mineral property, as thermal expansion. The two other quantities in equation (22) need to be evaluated using the elastic bulk modulus and function β estimated above. The resulting plastic volumetric strains are presented in Figure 12. Note that the values of plastic strain are not null at $c = 0$ per cent, due to prior consolidation due to seepage stresses and the application of the vertical load. For dioxane at zero external stress there is virtually no change in plastic strain below 70 per cent. A slight increase in plastic strain at $c = 70$ per cent qualifies that point as plastic, even through the effective stress is lower than that at 40 per cent. At 85 and 100 per cent the stress dropped nearly to zero, and at least part of this drop must have been accompanied by plastic strain. Most probably, the stress decreases faster than the yield surface at a lower c, given the fact that the amount of plastic strain at 85 per cent is almost identical to that at 100 per cent. Therefore, for the case of no nominal effective stress, the only point that corresponds to a continuous yielding at the given c is that a 70 per cent. For nominal stress of 40, 80 and 160 kPa the points at yield were for $c = 0$, 40 and 80 per cent, whereas for 100 per cent plastic straining was presumably interrupted, given the amount of drop in stress, associated with the increase of permability, Figure 12(a).

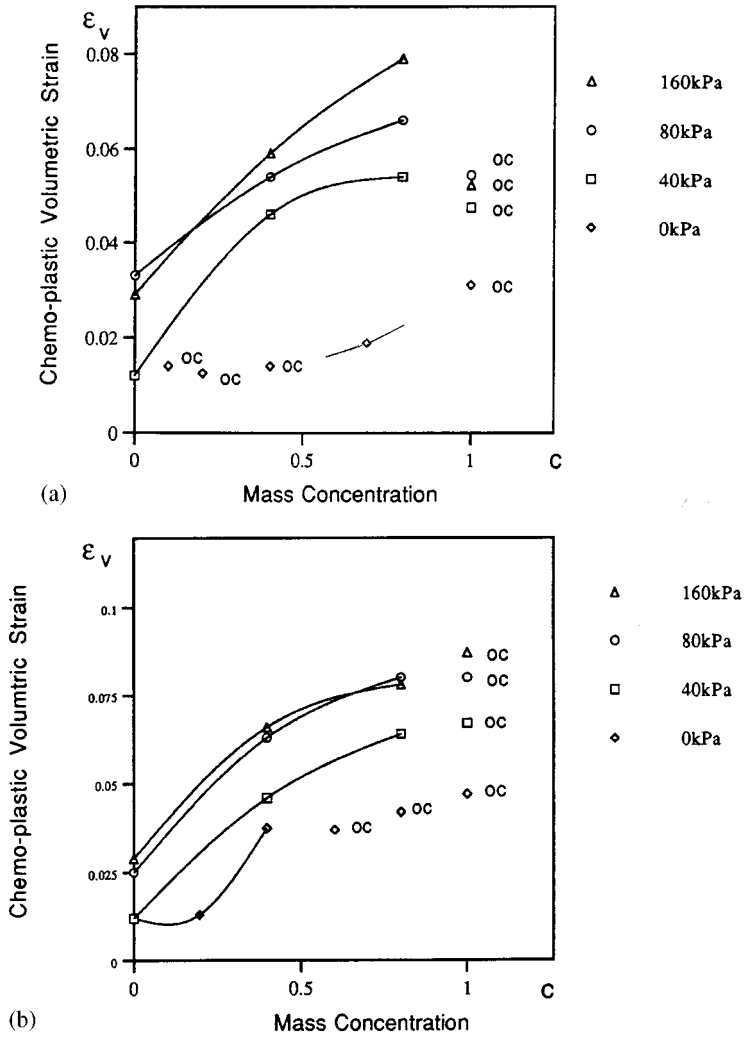

Figure 12. Chemo-plastic volumetric strain versus mass concentration. Points not joined by a line are in elastic (overconsolidated) stress state. (a) Dioxane at externally induced effective stress of 0, 40, 80 and 160 kPa; (b) ethanol at externally induced effective stress of 0, 40, 80 and 160 kPa

For ethanol, Figure 12(b), there is practically no change in plastic strain up to 20 per cent, at zero external stress and a very modest increase in effective stress due to seepage stress. A much more visible than for dioxane increase in plastic strain at $c = 40$ per cent qualifies that point as plastic, but already at $c = 60$ per cent any further increase in plastic strain is very limited. At higher external stresses the plastic strain development is similar to that for dioxane, except for $c = 100$ per cent data, which show a plateau or a modest increase in the plastic strain.

Knowing the amount of plastic strain and concentration for several points at a given apparant maximum precompression stress p'_{c0}, it is possible to determine the variation of the chemical softening for both permeants following equation (20). For the experiments of Fernandez and Quigley,[5,6] the calculated values of chemical softening function for both permeants are shown in

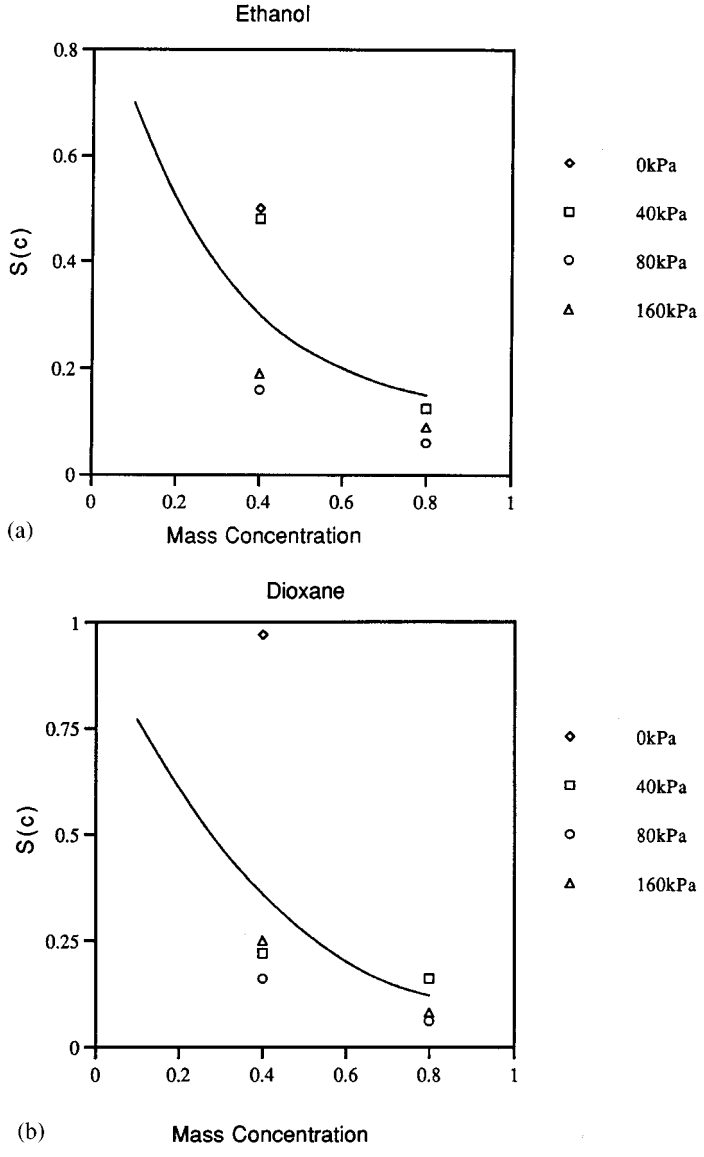

Figure 13. Chemical softening function $S(c)$ versus mass concentration for (a) ethanol, and (b) dioxane. (◇)-for 0 kPa, (□) for 40 kPa, (○) for 80 kPa and (△) for 160 kPa of external effective stress

Figure 13(a) and (b). Chemical softening is visibly sensitive to external effective stress: the softening is stronger at higher stresses. The most pronounced departure from the mean is for 'no external stress' case for dioxane. Part of the cause may be in neglecting the variation of plastic modulus λ with the contaminant mass concentration. However, since there is only one sure point at yielding for dioxane and two for ethanol to rely on, it would be unfounded to propose any specific rule of stress dependence on this basis. Thus, a stress insensitive, exponential chemical softening rule is interpolated between all the points available, separately for the two liquids.

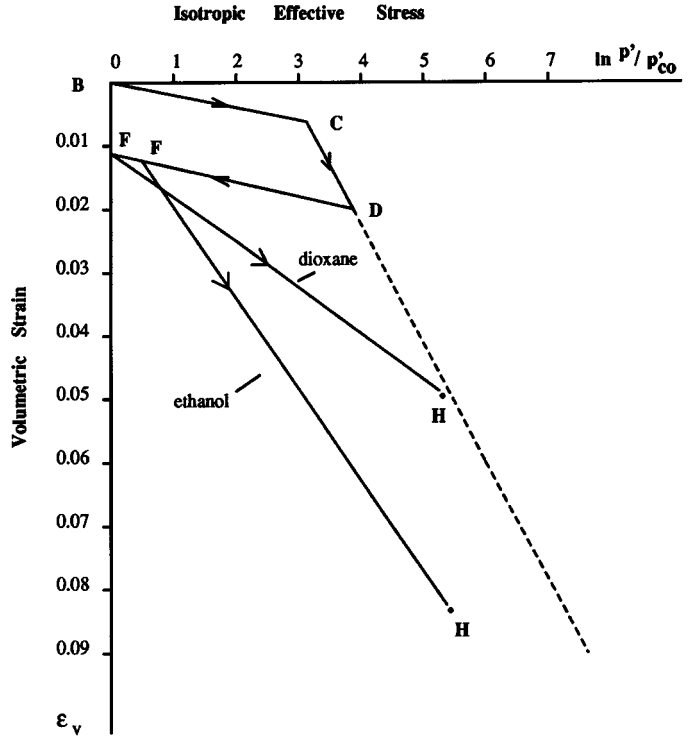

Figure 14. History of post-chemical damage loading of specimen permeated with ethanol and dioxane. B–C–D loading due to seepage forces during water flow, D–F corresponds to unloading due to seepage force drop and chemoplastic consolidation, F–H is plastic loading of contanminant permeated clay

The function of chemical softening is thus proposed as a simple exponential rule

$$S(c) = \exp(-ac) \tag{23}$$

where a is the chemical softening exponent, found to be 3·45 for ethanol and 2.78 for dioxane. It appears therefore that the chemical softening is weaker for dioxane, than for ethanol, which confirms the earlier observations.

As indicated before, in the above calculations the chemical sensibility of the plasticity modulus has been neglected. We shall now evaluate this sensibility quantitatively. Unfortunately, the values of seepage stress available from the experiments of Fernandez and Quigley[6] are only for the terminal cases of vertical external load at 290 and 302 kPa for ethanol and dioxane flows respectively. Note that the effective stress at 0 kPa of external stress, at 100 per cent of ethanol was only 5/2 and 3/2 kPa for dioxane, points F in Figure 7(a) and (b), due to greatly reduced seepage stresses related to the permeability increase. Moreover, at the end of the permeant exchange, the yield surface was significantly reduced to an unspecified amount, point G, so that the further loading and seepage process was initially elastic, FG, and became plastic at G, according to our hypothesis. Because of the lack of data concerning seepage stresses at intermediate stages, it was impossible to distinguish between elastic and plastic parts of the process. However, it may be speculated that the elastic portion of the process is very limited, and therefore negligible in the

modulus calculation. Thus, during the post-damage loading, the plastic process would start shortly after the beginning of the loading process reaching the final reported strain at the effective stress shown in Figure 14. All the intermediate stages were neglected in replotting in $\ln p'/p_0 - \varepsilon_v$ plane the data from the post-contamination compaction, Figure 6(a) and (b). It is easy to see that the effect of ethanol on clay was almost twice as strong as that on dioxane in terms of the change in the plastic deformability. If it is assumed that the portions FH for both contaminants are indeed linear, and the point of the onset of plasticity during this loading G is very close to F, it could be concluded that the plastic bulk modulus λ has changed from $\lambda = 0{\cdot}0324$ for water permeated clay, to $\lambda = 0{\cdot}0183$ for 100 per cent ethanol permeated clay, and to $\lambda = 0{\cdot}01197$ for 100 per cent dioxane permeated clay, assuming for both permeants the concentration insensitive $\kappa = 0{\cdot}00396$ and the value of the chemical softening function at 100 per cent contamination $S_e(100 \text{ per cent}) = 0{\cdot}031$ for ethanol and $S_d(100 \text{ per cent}) = 0{\cdot}062$ for dioxane. This indicates that the variation of plastic modulus with variable concentrations of the two contaminants is not insignificant. However, more data, including seepage stress, and possibly loading–unloading response to determine the position of the yield surface are needed to quantify the chemical softening and modulus chemical dependence as coupled effects.

CONCLUSIONS

A key question related to the studies on chemically induced changes in clay permeability is whether the effective stress typical of a relative geotechnical situation is sufficient to inhibit a major permeability increase. If the answer to this question is affirmative, the next question is whether the results obtained on the basis of flow pump experiments with high water pressure and high seepage stresses can be applied to field conditions, where the pressure and seepage stresses are very small.

The analysis presented indicates that the first question should be rephrased and asked in terms of chemically induced strains. Strain generated during laboratory contaminant flow in flow pump experiments such as those performed by Fernandez and Quigley[5, 6] were found to be either mechanical (due to seepage or external stresses), chemical (tendency to flocculate) or chemo-mechanical (chemo-consolidation) in nature. The first type of strains may be elastic (compressive or expansive) or plastic (compressive), the second ones are elastic (expansive), whereas the third kind is certainly plastic (compressive). Seepage stresses, generated in the experiments by the large specific discharge of the flow pump, are comparable or sometimes larger to the externally imposed stress. Their values, as opposed to the externally imposed stress are variable in time, since they depend on the material permeability, and in space, since they are equal to integrated seepage body forces. Because the role of effective stress in attaining plastic stress states is crucial, the variability of seepage forces was found to be a major difficulty in identifying the nature (reversible, or irreversible and seepage or chemistry induced) of strain. This is particularly important from the practical point of view, since the chemo-plastic strain controls the changes in permeability.

It should be realized that the large seepage forces do not occur in the field conditions, but may be a laboratory effect needed to ensure accuracy of permeability measurements. As such, they need to be taken into account in the analysis of the results as pointed out by Fernandez and Quigley[6] and the developed chemo-plasticity theory provides a tool for such analysis. Ideally, the experiments should be performed at low seepage stresses, so that their non-uniformity would not significantly after the constant effective stress distribution.

The mechanism of generation of chemo-plastic consolidation consists in the simultaneous occurrence of chemical softening, shrinking of the yield surface and plastic strain hardening which compensates for this shrinking, so that the effective stress remains in a plastic state. Thus, the necessary condition for the chemo-plastic consolidation is a sufficiently strong chemical softening. It was estimated to be the largest at concentrations around 70–80%. However, a subsequent drop in seepage stresses at 100 per cent have induced an unloading and interrupted the generation of chemo-plastic strain. In field conditions, where seepage forces are much smaller, the initial yield surface is expected to be much smaller. This would require, on one hand, a lower chemical softening, necessary to produce chemical consolidation, compared to the discussed experiments. On the other hand, the drop in the seepage component of the effective stress is expected to be significantly smaller, and thus, one may expect the chemical consolidation to occur also at the highest concentration of chemicals. Thus, its 'healing' influence on permeability may take place in field conditions as well. The experiments of Bowders and Daniel[21] seem to confirm this hypothesis. However, further experiments and numerical simulations using the developed model are needed to investigate a broader spectrum of conditions.

Several simplifying assumptions were made in this paper. The actual effective stress in clay is assumed to be uniform, while in the discussed experiments it remains unknown, and theoretically linear. In the phase of the low concentrations, the assumption of one-dimensional deformation probably holds. Therefore, especially during loading the K_0-state assumption is acceptable. However, when dehydration and possible opening of preferential channels occur, the lateral stress may change, and the effective stress path may be far from K_0-state assumption. Fernandez and Quigley[6] have seen no macroscopic and microscopic cracks, but other researchers repeatedly reported cracking due to clay permeation with organic chemicals.[20,22,23] However, it should be noted that occurrence of cracking depends on mineral, contaminant and stress conditions used in the experiments. From the mechanical point of view the chemical cracking, similarly to thermal cracking, is a result of kinematic boundary conditions in a boundary-value problem, and not only of tensile or shear strength as a constitutive property of the material per se.

The distinction between chemo-elastic strain and chemo-plastic consolidation strain, and the attribution of a purely elastic (reversible) character to the former one and a plastic (irreversible) character to the latter one need a confirmation which may be performed without flow. Such tests should first of all involve measurement of strain during transient contamination process, with $\dot{c} \neq 0$, and include the processes of rehydration, or replacement of contaminant with water, to asses possible reversibility of these processes.

As for the second question formulated at the beginning, the answer is that the presented model allows for a quantitative evaluation of chemical strains in any effective stress conditions, and thus allows one to evaluate the field situation on the basis of flow pump laboratory experiments.

Finally, from the discussed results it was concluded that a stronger chemical softening was induced in clay by ethanol than by dioxane. This observation differs from the one about permeability, which seems to be much more sensitive to dioxane than to ethanol.[5] From the point of view of the theory presented, these are coupled but separate phenomena. The former one depends on chemo-plastic strain and possibly on concentration-dependent deformational plastic modulus, whereas the latter one depends on the rate of desorption of bound water only. Since dioxane has a lower dielectric constant than ethanol, this would indicate that it is not the only characteristic controlling the discussed phenomena as suggested for much less dense clays, see e.g. Reference 19. An answer to this query should result from microstructural experiments and analysis.

APPENDIX

Table I. Degree of saturation, effective stress, and settlement for water-compacted samples permeated with ethanol–leachate mixtures (after Reference 6)

Ethanol(%)	Initial degree of saturation S_0 (%)[a]	Effective stress (kPa)			Final gradient i_f	Settlement (mm)	
		Initial	Final[b]			Static[c]	Seepage[d]
		σ'_{v0} (static)	σ'_{vf} (static)	J_{max} (seepage)			
0	100	0	0	159	810	0	0·446
20	95	0	0	225	1180	0	0·275
40	98	0	0	415	2285	0	0·591
60	100	0	0	195	1110	0	0·428
80	100	0	0	60	355	0	0·418
100	98	0	0	5	30	0	0·397
100	96	10	7.4	74	465	0·047	0·503
100	96	20	16	101	635	0·120	0·686
0	97	40	38	232	1180	0·080	0·353
40	98	40	36	641	3535	0·116	0·795
80	98	40	36	485	2880	0·132	0·820
100	98	40	35	344	2160	0·132	0·862
0	97	80	76	216	1095	0·357	0·507
40	98	80	75	543	2990	0·329	0·800
80	98	80	74	468	2775	0·348	0·922
100	97	80	74	441	2775	0·346	0·954
100	98	120	111	363	2285	0·476	0·869
0	100	160	152	278	1415	0·449	0·375
40	98	160	149	672	3700	0·473	0·727
80	98	160	148	689	4090	0·502	0·784
100	98	160	146	458	2880	0·692	0·772

[a] Initial degree of saturation calculated immediately following compaction and sample trimming to a thickness of 20 mm. Predamage stresses were then applied to the water-wet compacted samples prior to permeation with reference water (0·01 N $CaSO_4$).

[b] Final effective stresses refer to end of permeation with ethanol–leachate mixtures and reflect spring relaxation for σ'_{vf}.

[c] Static settlement for water-wet samples on application of σ'_{v0}.

[d] Seepage settlements are total settlements for initial reference water followed by pure leachate, pure ethanol, or ethanol–leachate mixture.

Table II. Degree of saturation, effective stress, and settlement for water-compacted samples permeated with ethanol–leachate mixtures (after Reference 6)

Dioxane(%)	Initial degree of saturation S_0 (%)[a]	Effective stress (kPa)			Final gradient i_f	Settlement (mm)	
		Initial	Final[b]			Static[c]	Seepage[d]
		σ'_{v0} (static)	σ'_{vf} (static)	J_{max} (seepage)			
0	100	0	0	159	810	0	0·446
10	100	0	0	120	606	0	0·424
20	99	0	0	127	635	0	0·366
40	98	0	0	178	880	0	0·267
70	99	0	0	130	635	0	0·190
85	100	0	0	6	30	0	0·193
100	95	0	0	3	15	0	0·177
0	97	40	38	232	1180	0·080	0·353
40	95	40	36	246	1215	0·265	0·674
80	97	40	36	282	1390	0·200	0·674
100	97	40	37	10	50	0·104	0·569
0	97	80	76	216	1095	0·357	0·507
40	95	80	75	258	1275	0·511	0·594
80	95	80	75	152	745	0·627	0·503
100	97	80	76	22	110	0·270	0·547
100	95	120	111	63	310	0·693	0·628
0	100	160	152	278	1415	0·449	0·375
40	96	160	148	366	1805	0·725	0·510
80	96	160	147	416	2045	0·782	0·635
100	97	160	153	30	150	0·450	0·339

[a] Initial degree of saturation calculated immediately following compaction and sample trimming to a thickness of 20 mm. Predamage stresses were then applied to the water-wet compacted samples prior to permeation with reference water (0·01 N $CaSO_4$).
[b] Final effective stresses refer to end of permeation with ethanol–leachate mixtures and reflect spring relaxation for σ'_{vf}.
[c] Static settlement for water-wet samples on application of σ'_{v0}.
[d] Seepage settlements are total settlements for initial reference water followed by pure leachate, pure dioxane–leachate mixture.

REFERENCES

1. G. Mesri and R. E. Olson 'Mechanisms controlling permeability of clays', *Clays and Clay Minerals*, **19,** 151–158 (1971).
2. D. E. Daniel, D. C. Anderson and S. S. Boyton, 'Fixed wall versus flexible wall permeameter', in *Hydraulic Barriers in Soils and Rocks*, **ASTM, STP** No. 874, pp. 107–126 (1985).
3. D. C. Anderson, K. W. Brown and J. C. Thomas, 'Conductivity of compacted clay soils to water and organic liquids' *Waste Management Res*., **3,** 339–349 (1985).
4. F. Fernandez and R. M. Quigley, Hydraulic conductivity of natural clays permeated with simple liquid hydrocarbons, *Can, Geotech J*., **22,** 205–214 (1985).
5. F. Fernandez and R. M. Quigley, 'Viscosity and dielectric constant controls on hydraulic conductivity of clayey soils permeated with water soluble organics'. *Can. Geotech J*., **25,** 582–589 (1988).
6. F. Fernandez and R. M. Quigley, 'Controlling the destructive effect of clay-organic liquid interactions by application of effective stresses' *Can. Geotech J*., **28,** 388–398 (1991).
7. J. K. Mitchell and M. Jaber, 'Factors controlling the long term properties of clay liners', in R. Bonaparte (ed.), in *Proc. ASCE Symp.* "*Water Containment Systems: Construction, regulation and performance'',* ASCE, 1990, New York, pp. 84–105..
8. R. K. Rowe, R. N. Quigley and J. R. Booker, *Clayey Barrier Systems for Waste Disposal Facilities*, Chapman & Hall, London, 1995.

9. T. Hueckel, 'Water mineral interaction in hygromechanics of clays exposed to environmental loads: a mixture theory approach', *Can. Geotech J*., **29,** 1071–1086 (1992).
10. T. Hueckel, 'On effective stress concepts and deformation in clays subjected to environmental loads', *Can. Geotech J*., **29,** 1120–1125 (1992).
11. T. W. Lambe, The structure of compacted clay', *J. soil mech. found. eng. div. ASCE*, **84,** 1654-1–1654-34 (1958).
12. T. H. Bennett and M. H. Hulbert, *Clay Microstructure*, IHRDC, Boston, MA, 1986.
13. K. Roscoe and J. B. Burland, 'On the genralized stress-strain behaviour of 'wet' clay, in J. Heyman and F. Leckie (eds), *Engineering Plasticity*, Cambridge Univ. Press, Cambridge, 1968., pp. 535–609.
14. R. E. Olson and G. Mersi, 'Mechanisms controlling compressibility of clays', *Proc. ASCE*, **SM6 96,** 1863–1878 (1970).
15. A. Sridharan and G. Venkatappa Rao, Mechanisms controllilng volume change of saturaed clays and the role of the effective stress concept. *Geotechnique*, **23,** 359–382 (1973).
16. T. Hueckel, 'Strain and contamination history dependence in chemo-plasticity of clays subjected to environmental loads', G. N. Pande and S. Pietruszczak, (eds.), *Numerical Models in Geomechanics*, A. A. Balkema, Rotterdam, 1995, pp. 329–336.
17. W. Prager, 'Non-isothermal plastic deformation', *Bol. Koninke Nederl. Acad. Wet*., **8,** 176–182 (1958).
18. T. Hueckel and M. Borsetto, Thermoplasticity of saturated soils and shales: constitutive equations, *J. Geotech. Eng*., **116,** 1765–1777 (1990).
19. S. Chen, P. F. Low, J. H. Cushman and C. B. Roth 'Organic compound effects on swelling and flocculation of Upton montmorillonite', *Soil. Sci. Soc. J*. A **51,** 1444–1450 (1987).
20. A. S. Abdul, T. L. Gibson, D. N. Rai, 'Laboratory studies of the flow of some organic solvents and their aqueous solutions through bentonite and kaolin clays' *Ground Water*, **28,** 524–533 (1990).
21. J. J. Bowders and D. E. Daniel, 'Hydraulic conductivity of compacted clay to dilute organic chemicals', *Proc. ASCE*. **113,** GT12, 1432–1448 (1987).
22. D. H. Gray, 'Geotechnical engineering of land disposal systems', in P. Baccin (ed.), *The Landfill*, Lecture Notes in Earth Sciences, No. 20, Springer, Berlin, 1989.
23. J. K. Mitchell and F. T. Madsen 'Chemical effects on clay hydraulic conductivity', in R. D. Woods (ed.), *Geotechnical Practice for Waste Disposal*', 87, GSP No. 13, 1987, pp. 87–116.
24. E. W. Brooker and H. O. Ireland, 'Earth pressures at rest related to stress history', *Can. Geotech. J*., **2,** 1–15 (1965).
25. D. E. Daniel, 'Landfills and impoundments', in (ed.) D. E. Daniel, *Geotechnical Practice for Waste Disposal*, Chapman & Hall, London, 1993, pp. 97–111.